Dorsal Fin in the White Shark, *Carcharodon carcharias*: A Dynamic Stabilizer for Fast Swimming

Theagarten Lingham-Soliar*

Department of Zoology, University of KwaZulu-Natal, Westville Campus, Durban 4000, KwaZulu-Natal, South Africa

ABSTRACT   Transverse sections of the skin in the dorsal fin of the white shark, *Carcharodon carcharias*, tiger shark, *Galeocerdo cuvier,* and spotted raggedtooth shark, *Carcharias taurus*, show large numbers of dermal fiber bundles, which extend from the body into the fin. The bundles are tightly grouped together in staggered formation (not arranged in a straight line or in rows). This arrangement of dermal fibers gives tensile strength without impeding fiber movement. Tangential sections indicate that the fibers in all three species are strained and lie at angles in excess of 60°. Of the three species investigated the dermal fibers in *C. carcharias* are the most densely concentrated and extend furthest distally along the dorsal fin. The overall results indicate that the dorsal fin of *C. carcharias* functions as a dynamic stabilizer and that the dermal fibers are crucial to this role. The fibers work like riggings that stabilize a ship's mast. During fast swimming, when the problems of yaw and roll are greatest, hydrostatic pressure within the shark increases and the fibers around the body, including in the dorsal fin, become taut, thereby stiffening the fin. During slow swimming and feeding the hydrostatic pressure is reduced, the fibers are slackened, and the muscles are able to exert greater bending forces on the fin via the radials and ceratotrichia. In *C. carcharias* there is a trade-off for greater stiffness of the dorsal fin against flexibility. J. Morphol. 263:1–11, 2005.   © 2004 Wiley-Liss, Inc.

KEY WORDS: white shark; dorsal fin; dynamic stabilizer; dermal collagen fibers; tensile tests

The white shark, *Carcharodon carcharias* (Fig. 1A), is the world's largest predatory fish (Randall, 1983; Compagno, 1984), reaching 7 m in length and weighing up to 2,100 kg (Froese and Pauly, 2002). Its locomotor pattern is categorized as thunniform (after that of the bluefin tuna, *Thunnus thynnus*), a form of swimming typical of some of the fastest marine vertebrates, e.g., scombrid fishes and cetaceans (Lighthill, 1975; Reif and Weishampel, 1986; Fish, 1998). Thrust in thunniform swimmers is largely restricted to the caudal oscillating hydrofoil, which minimizes body drag (Braun and Reif, 1985). The mean tailbeat frequencies in a typical thunniform swimmer, the kawakawa, *Euthynnus affinis,* are 4.57 and 7.03 Hz at swimming speeds of 40 cm s^{-1} and 80–100 cm s^{-1} respectively (Donley and Dickson, 2000). However, oscillations of the tail may induce recoil or lateral oscillations at the head. The latter could potentially diminish the net thrust by increasing viscous drag as the organism deviates from a rigid body (Nauen and Lauder, 2002; Fish et al., 2003). In *C. carcharias* there are two ways in which the anterior recoil forces may be reduced: narrow necking and streamlining of the caudal peduncle (Fig. 1A) by reducing the added mass effect posteriorly and corresponding recoil forces anteriorly (Blake, 1983; Webb, 1984; Reif and Weishample, 1986; Fish et al., 2003) and increasing the surface area around the center of mass via the dorsal fin (Webb, 1984), which increases the added mass and inertia at the anterior end of the animal (Fish et al., 2003). This reduces the forces of yaw (rotation about the vertical axis). Importantly too, the forces of roll (rotation about the longitudinal axis) are exacerbated in the mackerel sharks (Lamnidae), *Lamna nasus, Isurus oxyrinchus*, and *C. carcharias*, by the lack of ventral flattening of the head (contra most other sharks) (Thomson and Simanek, 1977), the rounded transverse-section continuing to approximately the mid-length of the body. Thus, the dorsal fin in *C. carcharias* (Fig. 1A) is also ideally located to resist roll.

Despite significant work on the tail mechanics of sharks (Alexander, 1965; Thompson, 1976; Thompson and Simanek, 1977; Wainwright et al., 1978; Graham et al., 1990; Ferry and Lauder, 1996), unfortunately there are few studies that have examined the various other body components of thunniform swimmers (Fish et al., 2003). As mentioned above, the dorsal fin in fast swimmers principally acts as a drag-based organ to reduce yaw and roll (Webb, 1984; Weihs, 1993; McGowan, 1999). Presence of a large, similarly shaped and similarly located dorsal fin in phylogenetically unrelated groups of cruising marine vertebrates (tuna, lamnid sharks,
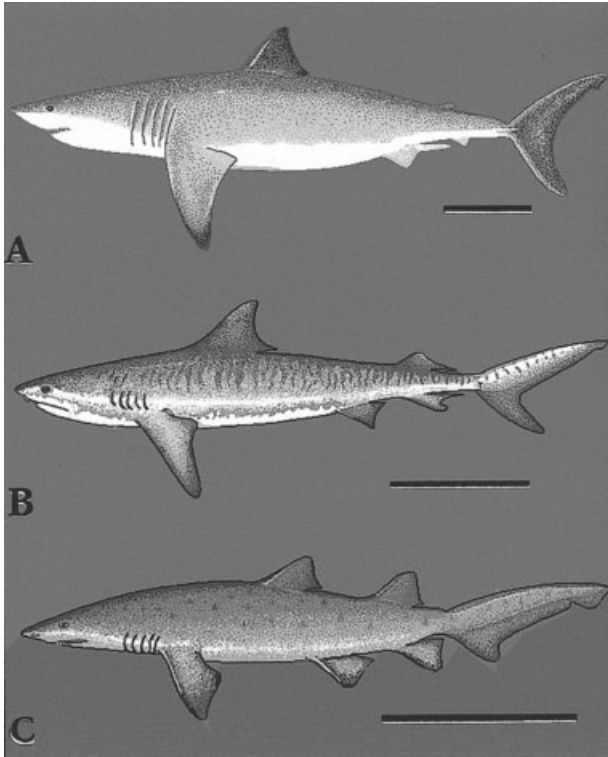
Fig. 1. Differences in body profiles in three sharks reflecting different lifestyles and swimming potentials. **A:** *Carcharodon carcharias*. **B:** *Galeocerdo cuvier*. **C:** *Carcharias taurus*. (Modified from Froese and Pauly, 2002.) Scale bar = 1 m.

dolphins (Delphinidae), and the extinct ichthyosaurs) underscores its importance as a stabilizer. Evolutionary constraints, however, have imposed notable differences in the anatomy and biomechanics of the dorsal fin in these groups. Within Teleostei, the dorsal fin in its derived condition, e.g., in fast-swimming perciforms, comprises two anatomically distinct portions: an anterior section supported by spines and a posterior section that is soft-rayed (Drucker and Lauder, 2001). The dorsal fin in dolphins is a de novo dermal structure, formed and supported only by connective tissue (Pabst, 1996a). In sharks, the dorsal fin consists of soft, cartilaginous radials and highly flexible fin rays or ceratotrichia (Gans and Parson, 1964). The dorsal fin in ichthyosaurs was also closely similar in shape to that of *Carcharodon carcharias,* although little is known of the internal anatomy (Lingham-Soliar, 2001). There is no evidence of either a bony or cartilaginous support but there is evidence of thick integumental fibers (Lingham-Soliar, 2001, and author's unpublished data).

For mobile animals, two functional requirements concern stability and maneuverability (Webb, 1984; Fish, 2002). Body designs that are adapted for stable movement are not suitable for high maneuverability and vice versa (Weihs, 1993), although compromises may be made between the two. An important consideration in functional design is the environment in

which the morphology operates (Fish, 2002). For example, the morphology of the dorsal fin of pelagic, fast-swimming dolphins reflects a body design that potentially favors stability in preference to maneuverability (Fish, 2002). It is possible to predict from this that animals such as *Carcharodon carcharias*, with a similar pelagic lifestyle and thunniform swimming mode, would polarize toward stable movement.

Previous studies have shown that the body of sharks is stiffened by numerous layers of collagenous fibers that wrap around the body in left- and right-handed helices (Motta, 1977; Wainwright et al., 1978). Among marine vertebrates similar fibers have been reported in the skin of eels (Hebrank, 1980), tuna (Hebrank and Hebrank, 1986), dolphins (Pabst, 1996a, 2000), and ichthyosaurs (Lingham-Soliar, 1999, 2001). Motta (1977) found that, in addition to presence in the body, a single layer of collagenous fibers also extends into the lower margin of the caudal fin of the Atlantic sharpnose shark, *Rhizoprionodon terraenovae*. Dermal collagenous fibers were not, however, investigated in the dorsal fin.

This study reports the gross morphology of the dorsal fin of *Carcharodon carcharias* and documents the histology of the dermal fibers. The histology of the dermal fibers of the slower-swimming sharks, the tiger, *Galeocerdo cuvier* (Fig. 1B), and spotted raggedtooth, *Carcharias taurus* (Fig. 1C), is also investigated. The present thesis is that the dorsal fin of *C. carcharias* is a dynamic stabilizer and that its effectiveness is achieved predominantly by masses of collagenous fibers continuing from the body into the dorsal fin. The mechanism may be analogized with riggings that stabilize a ship's mast. During fast swimming, when the problems of yaw and roll are greatest, hydrostatic pressure within the shark increases (Wainwright et al., 1978). Consequently, there is an increase in tension in the fibers around the body and in the dorsal fin.

MATERIALS AND METHODS
Materials

The shark species *Carcharodon carcharias, Galeocerdo cuvier*, and *Carcharias taurus* (Fig. 1) represent different lifestyles (Froese and Pauly, 2002) and swimming types (see Braun and Reif, 1985, and Lingham-Soliar and Reif, 1998, for analyses and definitions of the swimming types mentioned). *Carcharodon carcharias* (Fig. 1A) is a high-speed pelagic shark, primarily a coastal and offshore inhabitant of continental and insular shelves, and is a voracious feeder on generally large marine vertebrates (Cortés, 1999; Fergusson et al., 2000). *Galeocerdo cuvier* (Fig. 1B) is occasionally pelagic, making excursions in the open ocean, but is not a truly oceanic species (Tricas and McCosker, 1984). It has probably the widest diet range of all sharks (Tricas et al., 1981; Heithaus et al., 2001; Heithaus and Dill, 2002a, b). Its swimming type is carangiform (after that of fish in the family Carangidae). Carangiform swimmers have relatively flexible bodies and low-aspect-ratio tails, with much of the thrust derived from undulations of the posterior part of the body. Despite a reasonably fast swimming potential, much of *G. cuvier*'s time is spent in slow swimming. *Carcharias taurus* (Fig. 1C) is a

TABLE 1. Dermal fibers in the dorsal fin of three species of sharks

Shark species	Specimen no. length, stage of development, sex, wt.	Number of stratum compactum layers (based on bundles)	Thickness of stratum compactum (in mm)	Number of stratum spongiosum layers	Thickness of stratum spongiosum (in mm)	Range in sizes of bundles in stratum compactum (in microns). Largest and smallest chosen from ca. 30 bundles
Carcharodon carcharias	RBDS42 469.2 cm young adult, female, 1160 kg	A 10–12 B 10 C ?12 D 9–10 E ca. 4	A 1.8–2.0 B 4.3 C 4.0 D 1.8 E 0.5	A 12–14 B 8–9 C ? D ? E 6–7	A 1.2 B 1.0 C 1.0 D 1.4 E 0.7	A 180.2/270.5–330.6/1000 B 130/200.1–220.3/880 C 110.4/160.6–216.8/553 D 90.3/138.5–187.3/397 E 68.2/226–94.4/471.8
C. carcharias	RB 02057 191.0 cm, juvenile, female, 128 kg	A 9–10 B 8–9 C ca. 10 D 6–7 E 2	A 1.5 B 1.5 C 1.6 D 1.2 E 0.6	A12–14 B 8–10 C 8–10 D ? E ?	A 0.8–0.9 B 0.7 C 0.5–0.8 D 0.5 E 0.5	A 23.8/87.5–136.3/245.7 B 112.9/201.3–148/540.7 C 68.7/142.8–183.5/231 D 64.3/131.2–157.7/215.2 E 46.3/112.8–97.4/139.4
C. carcharias	Zin 02029 190 cm, juvenile, male, 120 kg	A 11–12 B 7–8 C ca. 8 D 4–5	A 2.0 B 1.5 C 1.0 D 0.9	A ca. 14 B ca. 14 C ca. 8–10 D ca. 7–8	A 1.0 B 1.1 C 0.8 D 0.8	A 74.6/116.9–300.4/803 B 121.1/159–220/680 C 50/60–170/250 D 44.6/56.3–101/195.3
Galeocerdo cuvier	HIB 02006 203 cm, young adult, female, 100 kg	A 7–8 B 4–5 C 2–3 D none	A 1.6 B 1.1 C 1.3 D 1.2	A 14 B 8–9 C ca. 6 D ca. 6	A 1.1 B 0.9 C 0.7 D 0.7	A 31.9/79–185.2/521.2 B 70/120–223.7/749.6 C 86.9/162–153.2/381.9 D none
G. cuvier	SUN01006 261 cm, adult, female, 164 kg	A 8–9 B 5 C 3–4	A 1.3 B 1–1.2 C 1.2	A 13–14 B 2 C 6–7	A 1.9 B 2.5 C 1.0	A 120/150.3–155/600.2 B 100/250–198/558 C 75.3/150.8–192.4/407.6
Carcharias taurus	208 cm adult, female, 202 kg	A 8 B 5 C none	A 1.9 B 1.0 C 1.5	A 9–10 B 9 C 7	A 1.1 B 1.1 C 1.0	A 153/179.3–301/483.2 B 70.1/120.9–217.4/333 C none
C. taurus	RB 02061, 205 cm, adult female, 140 kg	A 8–9 B 4–5 C none	A 2.2 B 0.85 C 1.7	A 10 B 10 C ca.8	A 1.1–1.2 B 1.1 C 0.9	A 130.4/212.1–279.9/552 B 73.7/113.9–285.7/336. C none

NB. A,B,C,D-E = point in the dorsal fin from which transverse sections were taken (see Fig. 2).

common demersal shark found inshore from the surf zone and in shallow bays to at least 191 m on the outer continental shelves, often on or near the bottom but also occurring in mid-water or at the surface (Last and Stevens, 1994). It feeds on shellfish, molluscs, and fish. Its swimming type is sub-anguilliform. Anguilliform swimmers are defined after the European eel, *Anguilla anguilla*, wherein all their forward thrust is derived from undulations that travel in waves along virtually the entire body. However, prey capture of faster-moving fish by *C. taurus* may include burst speeds involving a carangiform swimming mode (Last and Stevens, 1994).

Fresh carcasses of sharks caught in the protective gill nets off the KwaZulu-Natal coast by the Natal Sharks Board (NSB) (Cliff et al., 1996) were immediately transferred to deep freeze storage. The primary dorsal fins of three specimens of *Carcharodon carcharias*, two of *Galeocerdo cuvier* and two of *Carcharias taurus*, were removed for the histological preparations of the skin (Table 1). Caudal fins of the three species were also removed for comparative investigation of the fibers.

Histology

Five sites for the transverse sections of the skin were chosen at intervals along the dorsal fin of *Carcharodon carcharias, Galeocerdo cuvier,* and *Carcharias taurus*. (Fig. 2A shows the locations, A–E, of the five sections). All transverse sections (20 μ thick) were taken on the same plane, perpendicular to the skin surface and across the long axis of the fibers (Fig. 2B, arrow 1). Usually, four sections were made per site to ensure reliably accurate transverse sections of fiber bundles. Sites C and D represent areas closer to the leading and trailing edges of the fin, respectively.

Tangential sections (terminology after Hebrank, 1980, fig. 2) of 30−40 μ thickness from sites A–C were made using standard cryostat sectioning techniques. The sections lie on a plane parallel to the skin surface (Fig. 2B, arrow 2; also 2A, arrow 3), as opposed to transverse sections, and along the long axis of the fibers. A further tangential section was made on the boundary between the base of the dorsal fin and the body.

For comparative purposes, transverse and tangential sections were also made in the upper lobe of the caudal fins of the three shark species and on the caudal peduncle of *Carcharodon carcharias*. The relative positions of the sections in the different animals were obtained using a measurement grid (2 mm²).

Because of the toughness of the stratum spongiosum, in which the scales are embedded, a thin layer of the epidermis and dermis was scraped off in order to prevent creasing and distortion of the sections during microtomy. Paraffin embedding and Mallory's trichrome staining followed standard procedures (Humason, 1979). Transverse sections were examined and photographed using a Zeiss Axiophot light microscope and tangential sections using Differential Interference Contrast (polarized light).

Measurement data on the collagen fiber bundles[1] were obtained using a Panasonic Digital Biomed Analyzer. Thickness of fiber bundles in the stratum compactum was obtained from breadth and length measurements of ~30 bundles in each site. The range of sizes recorded (Table 1) represents the smallest and largest bundles of all bundles measured per site, per species.

---

[1]Type I collagen fibers, the most common type in vertebrates, are normally organized in bundles of fibrils (~80–90 nm thick), the structural unit of the fibers (Axer et al., 2001). The fibers, usually 8–10 μ thick, also occur in bundles or fascicles (Figs. 4, 5), frequently several hundred microns thick. These bundles are frequently referred to as fibers, which, strictly speaking, they are not, a point concurred with by Prof. Hubert Axer (pers. commun., 2003).
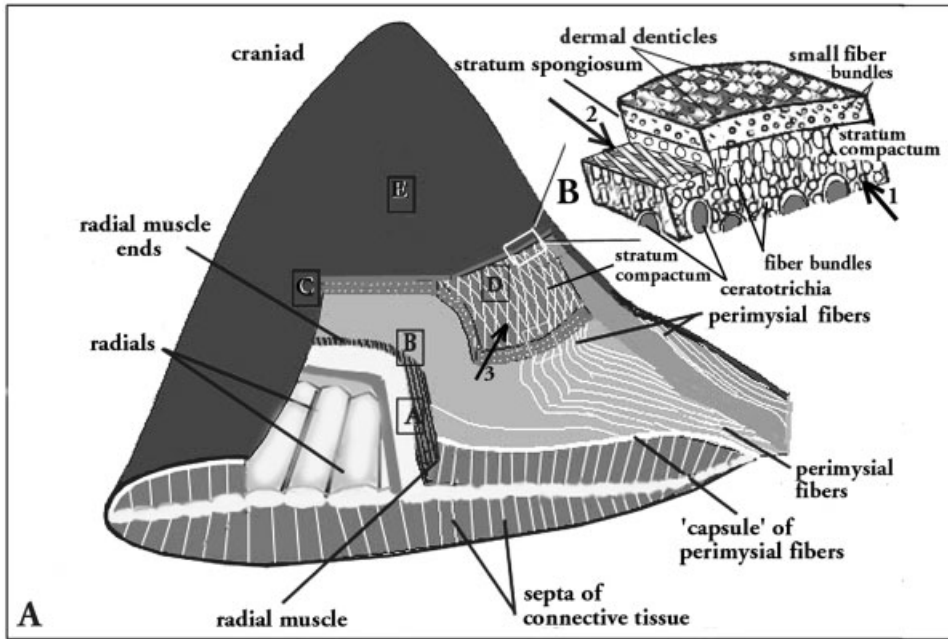
Fig. 2. Schematic representation of the dorsal fin of *Carcharodon carcharias*. **A:** The rectangle inserts A–E show sites from which transverse-sections of the skin were taken (see Table 1 and Figs. 4, 5). Note, sites A–E appear in this figure for convenience and represent only the locations of the dermal sections and are not intended to represent different orientations, levels, etc. Tangential sections were taken from sites A–C. Arrow 3 shows fibers in tangential view. **B:** Representative transverse sections of the dermis taken identically in all five sites (A–E). Arrow 1 shows the plane of the transverse sections and arrow 2 the plane of the tangential sections.

Dissection of the dorsal fin of *Carcharodon carcharias* (Fig. 3) was made prior to removal from the animal to avoid distortion or slackening of fibers and muscles.

RESULTS
Subdermal Tissue of the Dorsal Fin

In *Carcharodon carcharias,* sheaths of perimysial connective tissue (PCT) enter the dorsal fin from the body (Figs. 2, 3). Part of the PCT attaches to the base of the dermis (Figs. 2, 3A, in the latter figure, see within white quadrate).

The radial muscles extend less than half way up the dorsal fin and attach to the cartilaginous radials (Fig. 3A, arrow 2). Perimysial fibers from other parts of the body attach to the dorsal fin radials (arrow 1), although indirectly via a dense connective tissue sheath (CTS) or "capsule" formed by the fibers wrapping around the radial muscles (Figs. 2A, 3A, arrow 1). Perimysial fibers (Fig. 3B, arrow 4; 3C, arrow 5) also attach to the dorsal septum of connective tissue (Fig. 3C, arrow 6). An analogous system of connective tissue to that of the dorsal septum of sharks was recently noted in ichthyosaurs (Lingham-Soliar, 2001). Masses of connective tissue traverse the body musculature (Fig. 3C, arrow 7; detail Fig. 3D) and numerous septa of connective tissue connect the radial muscle to the radials (Fig. 3C, arrow 8).

Dermal Tissue of the Dorsal Fin
Stratum compactum transverse sections.

Carcharodon carcharias. In specimens RBDS42 and ZIN 02029 the collagen fiber bundles are elongated in transverse section, of varied size, and staggered in formation. The term "staggered" is used here to define fiber bundles that are not clearly demarcated in rows or arranged in a line in transverse section, but rather a state in which bundles of varying heights are somewhat interdigitated (Fig. 4A,B). This is in contrast to bundles occurring in neat rows (frequently separated by septa) as revealed in the dermis overlying the body of sharks by Motta (1977) and in the caudal fin. An exception was found in site A of *C. carcharias*, specimen RB 02057 (Fig. 5A), in which the fiber bundles occur in rows separated by connective tissue. However, a further section ~0.5 cm distally from the previous showed the typical staggered formation of stratum compactum fiber bundles (also see Fig. 5B,C) of the dorsal fin (the transition from the layered to the staggered fiber bundle arrangement occurs fractionally later in this specimen; see below). Since counting of rows is in most cases impossible, instead an approximate count is provided of the number of bundles (interpreted as layers) that are more or less stacked one upon the other from the base of the stratum compactum to the top.

The concentration of fiber bundles in the dorsal fin of *Carcharodon carcharias* is high, with densely populated fiber bundles occurring in sites A–D (Figs. 4A,B, 5A–C), and many fiber bundles extending to the furthest point of the dorsal fin examined, site E (Fig. 5D). In site E, however, the orientation of the bundles changes, with the greatest dimension lying on the horizontal rather than vertical plane.

Galeocerdo cuvier. In *Galeocerdo cuvier,* fiber bundle structure and organization (Fig. 5E) coincide fairly well in the lower regions of the fin with that of *Carcharodon carcharias*. At site A the concentration of stratum compactum fiber bundles is similar to that of *C. carcharias*. However, from
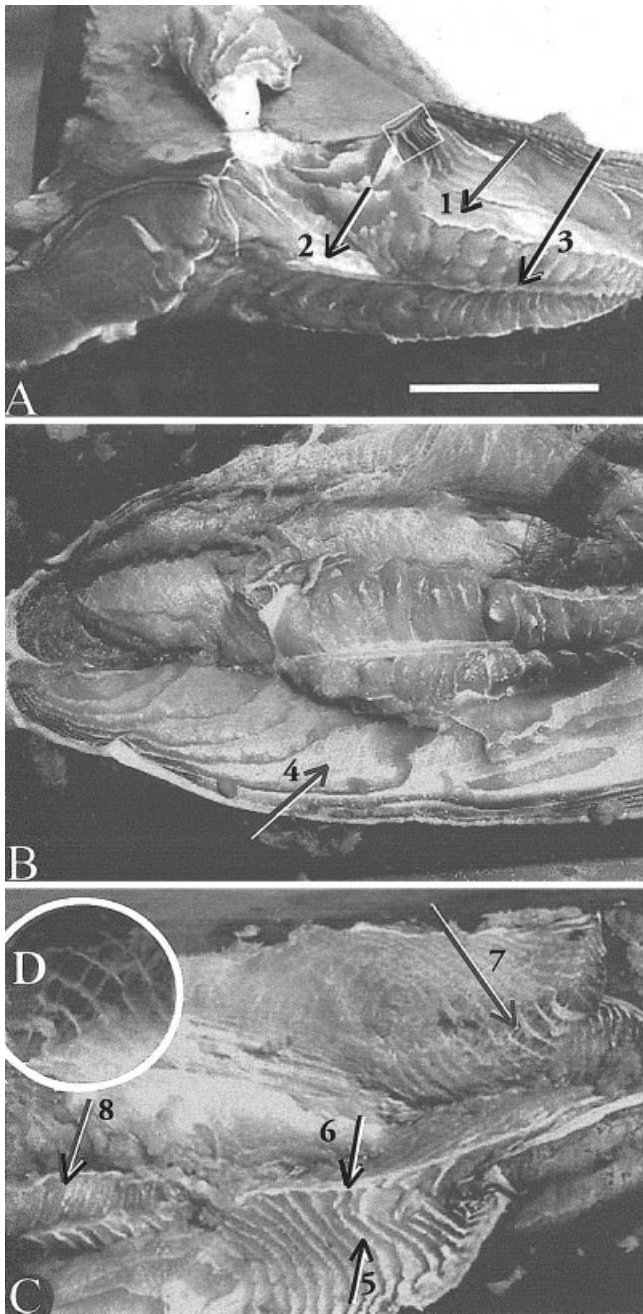
Fig. 3. Dissection of the dorsal fin of *Carcharodon carcharias*. **A:** Layers of perimysial connective tissue form a capsule of connective tissue around the radial muscles (arrow 1); perimysial fibers also attach to the connective tissue at the base of the compact dermal fibers (indicated by white quadrate). Toward the center of the figure a segment of radial muscle is removed to show connective tissue attaching a capsule of connective tissue to the fin radials (arrow 2); these attach at virtually 90° to the long axis. Arrow 3 shows the radials. Scale bar = 25 cm. **B:** Dissection with most of the dorsal fin removed and showing sheaths of perimysial fibers attaching to the body surface and to the dorsal fin (arrow 4 shows layers of alternately left- and right-handed oriented fibers). **C:** Dorsolateral dissection of area around the dorsal fin. In the posterior region of the dorsal fin (right) along the mid-dorsal ridge the perimysial connective tissue (arrow 5) attaches to the dorsal skeletogenous septum (arrow 6). Along the top of the picture thick bundles of helical fibers that make up the connective tissue sheaths can clearly be seen (arrow 7). Left, radial muscles connected by connective tissue septa (arrow 8). **D:** Inset, detail of area indicated by arrow 7.
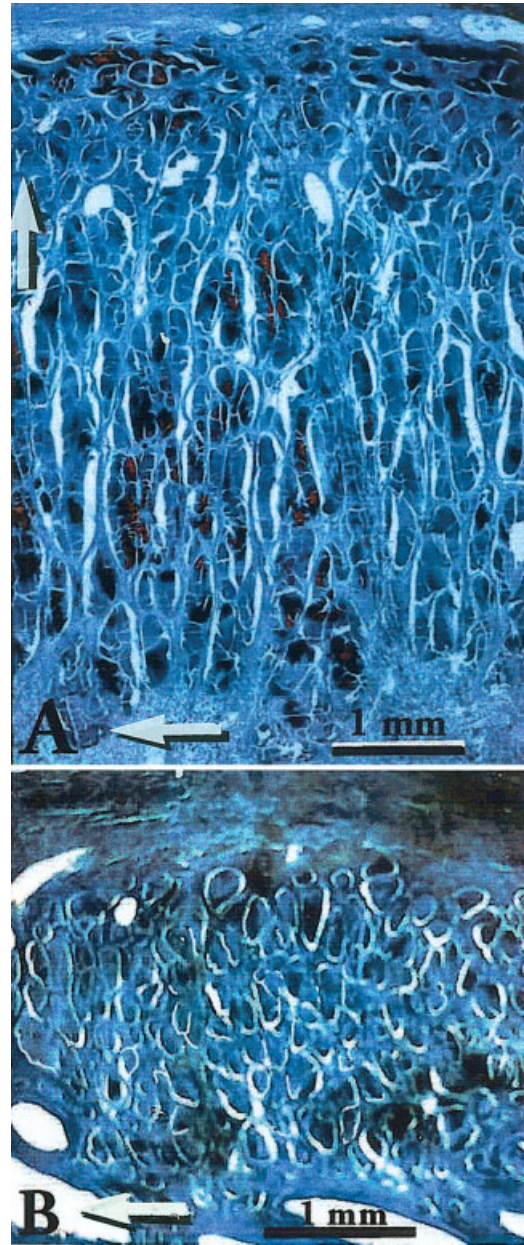

Fig. 4. Transverse sections of the dermis of the dorsal fin of *Carcharodon carcharias*, RBDS42 (female). **A:** Site A shows the thick stratum compactum with densely packed fiber bundles in staggered formation. Above, the stratum spongiosum is evident, while at the bottom part of the connective tissue layer can be seen. Note, ceratotrichia are not present in this region. **B:** Even at site D, close to the trailing edge of the fin, the stratum compactum fibers are still densely arranged. The fiber bundles are relatively less elongated, probably a consequence of a decrease in skin thickness. Large spaces at the base of the section were left by ceratotrichia. Scale = 0.5 mm.

this point on the fiber bundles are sparser and virtually cease beyond site C.

Carcharias taurus. Fiber bundle structure and staggered arrangement coincide with that of the above species at site A (Fig. 5F). Most notably in this species, the concentration of fiber bundles decreases rapidly from the lower part of the fin distally. Only
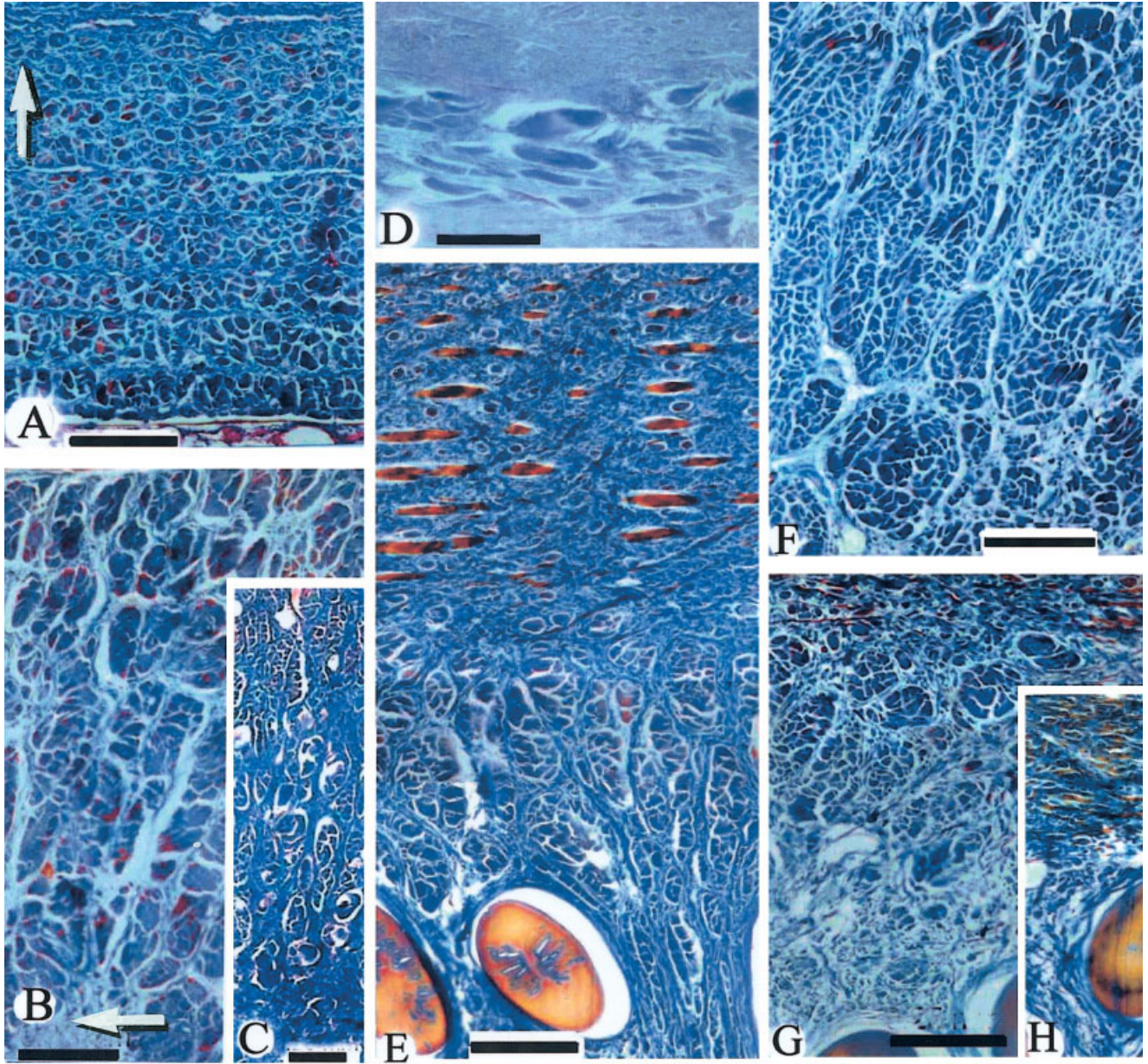
Fig. 5. Representative transverse sections of the skin from the dorsal fin of *Carcharodon carcharias, Galeocerdo cuvier,* and *Carcharias taurus*. All sections are taken from the skin surface downward as illustrated in Figure 2B and with similar orientations (see Materials and Methods). Arrows at the upper and lower parts of the figure show top and craniad directions of the sections, respectively. **A:** Section from site A of *C. carcharias* RB 02057 (female) in which approximately nine distinct rows of dermal fiber bundles are present (compare Figs. 4A, 5B). Just visible above is the stratum spongiosum and at the bottom the connective tissue layer in which collagen fiber bundles are absent. **B:** Site A of *C. carcharias* ZIN 02029 (male) in which the dense fiber bundles are staggered in formation. **C:** Part of the stratum compactum of *C. carcharias* RBDS42 at site C in which numerous layers of fiber bundles are present. **D:** About four rows of stratum compactum fibers are seen at site E in *C. carcharias* RBDS42. The fiber bundles have oriented with the long axis along the horizontal plane. Above is the stratum spongiosum and at the bottom connective tissue. **E:** Site B in *Galeocerdo cuvier* in which the fiber bundles of the stratum compactum are already reduced. The upper half of the picture shows the stratum spongiosum in which small bundles of fibers occur within a collagenous matrix. The large yellow inclusions toward the bottom are ceratotrichia. **F:** A major part of the stratum compactum fibers of *Carcharias taurus* RB 02061 at site A showing densely aggregated fiber bundles in staggered arrangement. **G:** By site B the stratum compactum fibers have dwindled to 2–3 rows. Above is the stratum spongiosum and below connective tissue with ceratotrichia just in view. **H:** At site C there are no stratum compactum fibers in *Carcharias taurus* RB 02061; only small fiber bundles may be seen in the stratum spongiosum. Scale bar in all figures except **D**, 0.25 mm. Scale bar in **D**, 0.5 mm.
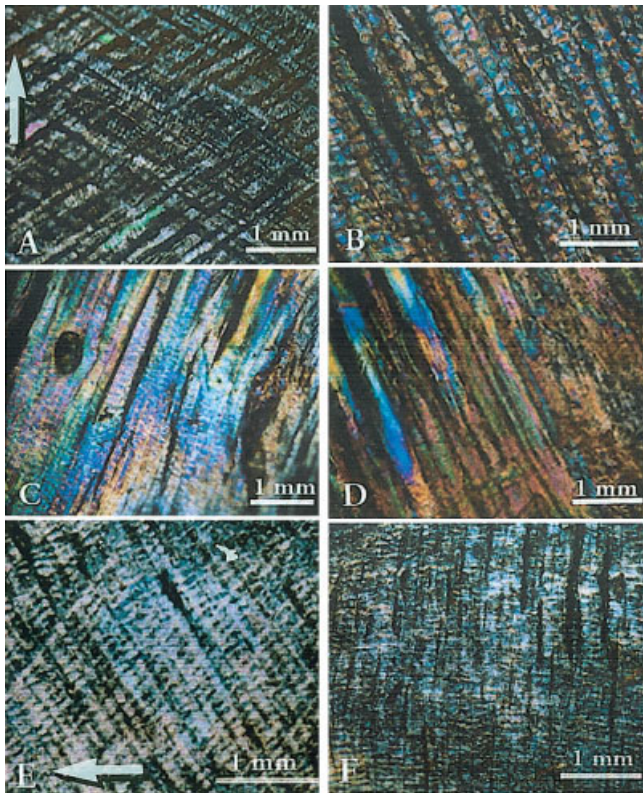
Fig. 6. Tangential sections of stratum compactum fibers of *Carcharodon carcharias, Galeocerdo cuvier*, and *Carcharias taurus* (sectional areas were large, ~2.5 × 1.5 cm). Arrows at the top and bottom show dorsal and craniad directions of the sections respectively. **A:** Section just below the dorsal fin of *C. carcharias*. Fibers are in left and right-handed orientations of ~40° to the long axis and form an orthogonal meshwork. **B–D:** Fibers at site A in all three species. The fibers form thick bundles and are oriented at 60°+ to the long axis of the shark. In **B**, the subdivision of the thick fiber bundles into smaller fiber bundles is clearly distinguishable along this different plane. Apparent breaks in fiber continuity are actually minute creases of the fibers which are better distinguished under different azimuths of polarized light. The fibers continue with approximately the same density and angles (60°) in *C. carcharias* to at least site C. **E:** Fibers in the stratum compactum of the caudal peduncle of *C. carcharias*, oriented at angles of 60°+ to the long axis, form an orthogonal meshwork. **F:** Fibers in the stratum compactum of the lower third–half of the upper lobe of the caudal fin of *C. carcharias* are densely arranged and oriented parallel to the lobe. The differences in fiber pattern compared with A (body) and E (caudal peduncle) are striking.
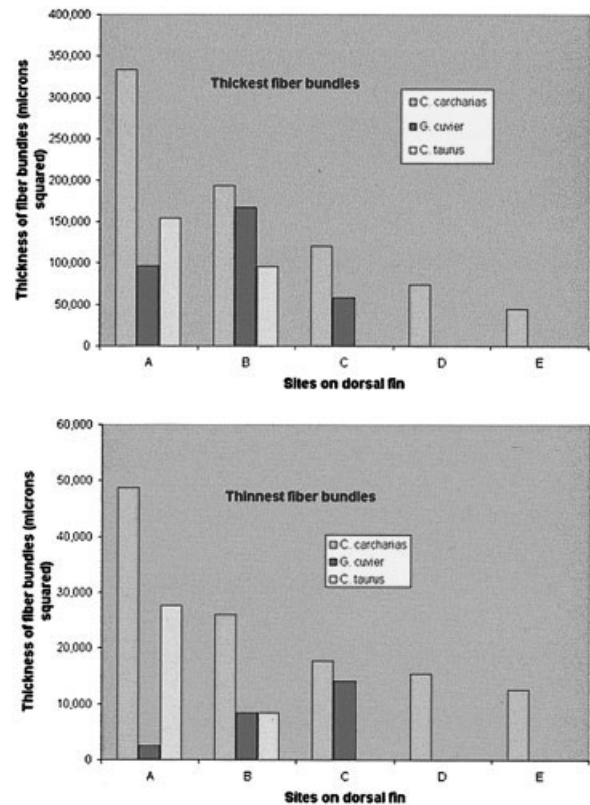

Fig. 7. The thickest (**A**) and thinnest (**B**) fiber bundles found in representative sections of the stratum compactum of the dorsal fin of *Carcharodon carcharias, Galeocerdo cuvier,* and *Carcharias taurus*.

about half the number of stratum compactum fiber bundle layers are found in site B of the fin (Fig. 5G) compared with the same region in *Carcharodon carcharias*. In site C and further up the dorsal fin the stratum compactum fiber bundles are absent and stratum spongiosum fiber bundles only are present (Fig. 5H, inset; Table 1, Fig. 7).

Stratum compactum tangential sections in the three species investigated. Observations on the tangential sections of the stratum compactum of the three shark species (Fig. 6) complement those obtained from the transverse sections. The fiber bundles at the boundary between the fin base and body are oriented at angles of ~40° to the long axis, with the left- and right-handed helical configuration of the orthogonal meshwork evident (Fig. 6A). However, the angles change rapidly to 60–65° to the long axis (all species) near the base of the fin, which is maintained (where fibers are present) throughout the sections examined. The fiber bundles are much thicker and denser than anywhere else examined in the three species and are more closely organized (Fig. 6B–D; Table 1), in contrast to those of the body (Motta , 1977, table 3). A number of successive tangential sections into the stratum compactum show several, apparently consecutive layers of fiber bundles oriented in the same direction, rather than in alternating left- and right-handed orientations. In other layers, alternating left- and right-handed orientations of fiber bundles occur, forming an orthogonal meshwork. In all cases the fibers are steeply oriented (60°+ to the longitudinal axis).

The number of layers and the range in sizes between the smallest and largest fiber bundles (measured as width/length) for all three species are given in Table 1 and Figure 7.

Stratum spongiosum. In contrast to fiber bundles in the stratum compactum, those in the stratum spongiosum of all species examined are
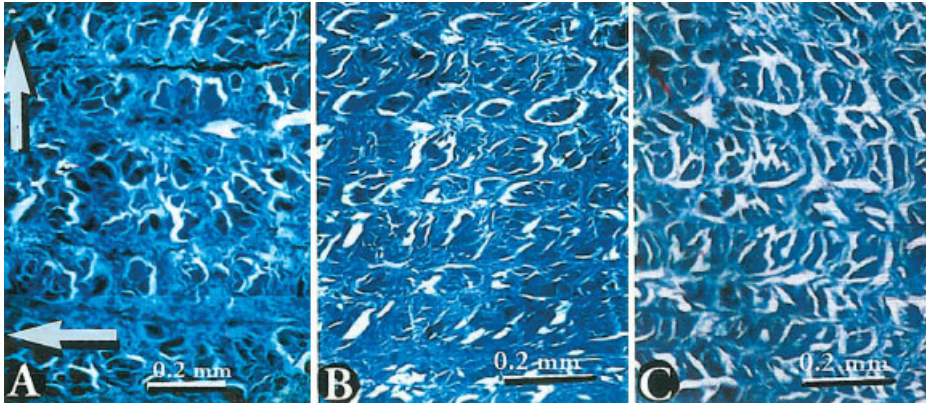
Fig. 8. Transverse sections of the dermis of the caudal fin (lower third – half of upper lobe) showing fiber bundles arranged in distinct rows. **A:** *Carcharodon carcharias.* **B:** *Galeocerdo cuvier.* **C:** *Carcharias taurus.*

sparser, small, and more or less organized in rows within a connective tissue matrix (Fig. 5E, top, Table 1). Grouping of the bundles is rare. The size ranges are not remarkably different in all three species, varying from a minimum size of 9.8/21.7 to a maximum of 45.1/70.2 μ (data not included in table).

Dermal Fibers in the Stratum Compactum of the Caudal Fin

It is particularly striking that, unlike in the dorsal fin, but as in the dermis overlying the body of sharks (Motta, 1977), transverse sections show that the fiber bundles of the stratum compactum in the caudal fin occur in well-ordered rows in all three species (Fig. 8). Tangential sections of the dermis of the caudal fin of *Carcharodon carcharias* clearly show that these fiber bundles extend parallel to the long axis of the upper caudal lobe (Fig. 6F), in contrast to the condition of the fibers over the body (Fig. 6A) and in the caudal peduncle (Fig. 6E), which are alternately left- and right-hand oriented to form an orthogonal meshwork. This condition is treated cautiously until more specimens are examined.

DISCUSSION

The present study indicates the presence of dermal collagenous fibers in the dorsal fin of sharks, contrary to the view of Moss (1972) that only a basement membrane is present, the dermis being absent. To gain an understanding of the functional role of such fibers in the dorsal fin, I analyze some of their biomechanical and structural properties. The findings in all but the last point in the summary below, preceding the discussions, refer to the stratum compactum: 1. In all species the fiber arrangements of the dorsal fin occur in staggered formation, generally contrasting with the well-ordered rows previously found in the dermis overlying the body of the sharks. 2. Fibers are grouped in bundles of varying sizes, somewhat resembling skeletal muscle fasciculi. 3. Variations were found in stratum compac-

tum fiber bundle profiles and densities in the three species with the most impressive concentration, distribution, and number of fiber bundle layers occurring in *Carcharodon carcharias*. 4. Fiber angles in the dorsal fin in the three species are 60°+ to the long axis. 5. In the dorsal fin in all three species an orthogonal meshwork is formed by some layers of fibers but not by others. 6. Fiber bundles at the boundary just below the base of the dorsal fin are smaller in diameter and form an orthogonal meshwork. 7. In the caudal fin in *C. carcharias* fibers extend in parallel formation along the length of the dorsal fin in a number of clearly demarcated layers or rows. 8. In *C. carcharias* the fiber bundles in the caudal peduncle (close to the caudal fin) occur at angles in excess of 60° to the long axis of the animal. Fibers in layers are alternately left- and right-hand oriented and form an orthogonal meshwork. 9. In the stratum spongiosum the fiber bundle profile (small size, sparse, and not grouped in larger bundles) is generally similar in all three species.

Functional Implications of the Fiber Architecture in the Dorsal Fin

Distinct rows of fiber bundles in a similarly confined area of the caudal fin (Fig. 8) indicate that the staggered arrangement of the fiber bundles in the dorsal fin is not solely a consequence of restricted space. Rather, functional explanations related to the mechanics of a dynamic stabilizer are proposed. For instance, irregular, interwoven bundles of fibers, frequently found in the skin of many animals, confer great strength to the skin (Vincent, 1990; Vincent et al., 1991; Burkitt et al., 1993), as do cross-over fibers present in some layers of shark skin (Motta, 1977; Wainwright et al., 1978). However, such configurations impede the movement of the fibers along a specific plane, given that fiber movement may be important in, e.g., the reorienting of fibers toward the stress axis, as Naresh et al. (1997) have shown in tensile tests on the skin of *Carcharias laticaudas*. On the other hand, mechanical stiffness may also be achieved by prestressing of collagenous fibers (Veronda and Westman, 1970; Gordon, 1978). In the
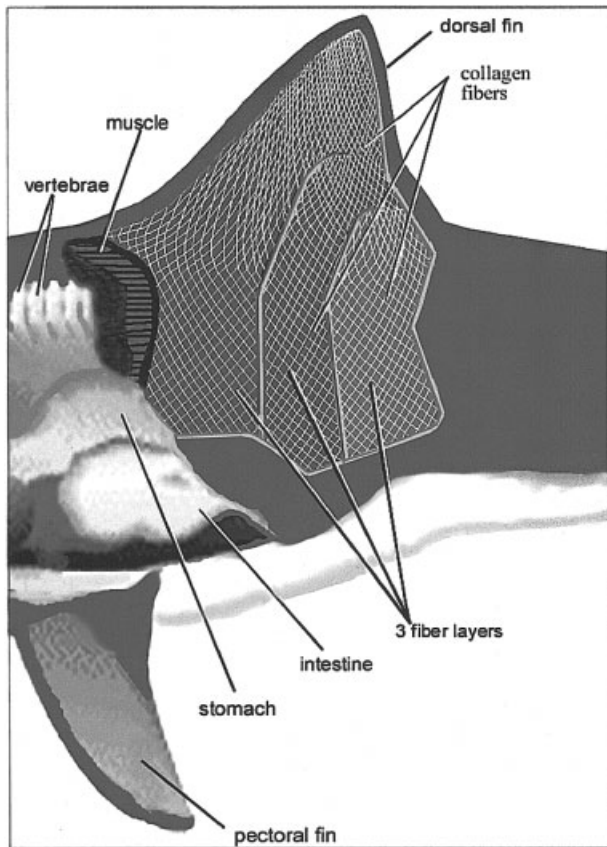
Fig. 9. A schematic view of the dermal fibers extending from the body into the dorsal fin of *Carcharodon carcharias.* The angles become much steeper in the dorsal fin (60°+) and the orthogonal meshwork is not always as evident as depicted in the scheme.

dorsal fin there appears to be a compromise, allowing an increase in tensile strength but without impeding the transfer of fiber tension from the body (Fig. 9). This is achieved principally in two ways: fiber bundles are tightly packed in transverse section in more or less staggered formation (like bricks in a wall) but without being interwoven either as bundles or layers; and fiber bundles are steeply oriented (in excess of 60°) and strained (or prestressed), facilitating rapid transfer of tension from the body (see below).

The mechanical characteristics of the dorsal fin are directly related to the peculiarities of the collagenous fiber architecture described above and to the cross-helical fibers wound around the body of the shark. In a cylinder the hoop stress is equal to longitudinal stress with, the cross-helical fibers wound at 55° 44″ (Wainwright et al., 1976; Alexander, 1987). In sharks, however, the angles vary between 50–70° in different regions of the body. Differences in the meshwork character of the collagen architecture of sharks (Motta, 1977; Wainwright et al., 1978) and dolphins (Pabst, 1996a) confer specific dynamic properties that allow deformation less or more before the fibers themselves come under substantial

strain (Wainwright et al., 1976, 1978; Axer et al., 2001; Drucker and Lauder, 2001). High fiber angles (relative to the longitudinal axis) in the dorsal fin are construed to allow less deformation of the fiber architecture and consequently a rapid transfer of tension from fibers wound around the shark's body. It is envisaged to be particularly effective when there is a significant increase in internal hydrostatic pressure during fast swimming.

A further function for high fiber angles of collagenous fibers in the dorsal fin of the sharks under study, that of reinforcement, is considered. Pabst (1996a) suggested that very high fiber angles in collagenous fibers in the caudal peduncle of dolphins served to reinforce the peduncle, in that case to act like a flexor retinaculum to keep the lateral tendons from bowstringing. A further prediction of her model (Pabst, 1996a, p. 49) is that the skin in the caudal peduncle of lamnid sharks would also have a retinacular function, and that the skin fiber angles would be higher than those reported for slower-swimming sharks (45–50°) lacking a caudal peduncle. The present findings support the prediction and show skin fiber angles in the caudal peduncle of *Carcharodon carcharias* in excess of 60° to the long axis (Fig. 6E).

The dynamic mechanism by which the dorsal fin of *Carcharodon carcharias* is stiffened can be likened to that of the riggings that stabilize the mast of a sailing ship (Fig. 9). In the lemon shark, tension on the shark's skin due to internal hydrostatic pressure was shown to increase with speed from ~20–35 kN m^{-2} to 200 kN m^{-2} (Wainwright et al., 1978). This tension is transferred to the fibers on either side of the dorsal fin, which results in the fin becoming rigid. Thus, maximum stiffness occurs with maximum speed, and it is no coincidence that this also occurs when the problems of yaw and roll are most serious. Wainwright et al. (1978) also found that while swimming slowly the shark bent its body in right and left bends of 38 cm radius of curvature, and during bursts of fast swimming bends of 20 cm radius were produced, and that the pressure rose on both the concave and convex sides of the fish. This is important since it ensures that the pull on either side of the dorsal fin is identical. Indeed, it is unlikely to be otherwise in *C. carcharias*, given the location of the dorsal fin at the stiffest part of the shark's body, where its girth is greatest and significant undulations are unlikely.

The high concentration of fibers in the skin of the dorsal fin is in most respects similar to that of the caudal fin in *Carcharodon carcharias*. In view of these similarities, the test Wainwright et al. (1978) performed to assess the torsional role of the collagenous fibers conveyed to the shark's body is considered relevant to the relationship between the fibers of the shark's body and the dorsal fin. The authors first twisted the intact tail (clamped to a board) about the shark's axis and found that a 40% twist required a 4.8 N-m torque. However, the same twist

after the skin was cut around the base of the tail required 2.4 N-m. This high passive resistance was achieved despite the low percentage thickness of skin relative to muscle (tensile tests on the dorsal fin of *C. carcharias* showed virtually identical results; author's unpublished data). It seems reasonable to conclude from this that skin in the dorsal fin of the great white shark, with masses of collagenous fibers, must likewise play a dominant part in stiffness against bending and twisting forces and that in the pressurized shark it would be even greater.

While the functional importance of dermal collagenous fibers in the dorsal fin of sharks cannot be overemphasized, the role of perimysial fibers in strengthening the fin around the radial muscles and in controlling the movements of the dorsal fin should not be overlooked (coinciding with observations in other parts of the body of sharks; J.J. Willemse's pers. commun. in Motta, 1977, p. 457). The indirect attachment of the capsule of perimysial fibers via numerous septa of connective tissue to the fin rays at virtually 90° to their surface (Figs. 2A, 3C) presumably averts undue torque (twisting of the fin) that might otherwise arise from muscle fibers originating from a number of different directions.

The fibers in the various rows in the caudal fin extend parallel to the long axis of the upper lobe of *Carcharodon carcharias*, as demonstrated by several tangential sections (Fig. 6F). Parallel or steeply oriented fibers would presumably facilitate rapid transfer of tension to the fibers in the caudal fin. The implications are of fibers acting as elastic springs in the caudal fin of *C. carcharias*. However, the subject of elastic springs and conservation of energy is a complex and controversial topic (Bennet et al., 1987; Fish and Hui, 1991; Blickhan and Cheng, 1994; Pabst, 1996b) and warrants further investigation. The present findings suggest a possible line of investigation.

Ecological Consequences of a Dynamic Dorsal Fin

A highly stiffened dorsal fin is necessitated by the lifestyle of *Carcharodon carcharias*, a pelagic, high-speed swimmer at the top of the marine food chain (Randall, 1983; Boustany et al., 2002; Froese and Pauly, 2002). This lifestyle contrasts with that of *Carcharias taurus* and *Galeocerdo cuvier*. The more posterior position of the dorsal fins in *C. taurus,* compared with *C. carcharias* and *G. cuvier* (see Fig. 1), which is exemplified in fish such as the northern pike, *Esox lucius* (Webb, 1983; Webb and Weihs, 1983), may enable more rapid acceleration from a stationary position compared with slower starts in thunniform sharks (McGowan, 1999). This feature is useful in ambush predation. A special ability to control its buoyancy and remain motionless by gulping air into the stomach (Bass and Ballard, 1972) may also contribute to predation by stealth. *Galeocerdo*

cuvier spends considerable time swimming slowly in habitats that are varied (Tricas et al., 1981; Heithaus et al., 2001; Heithaus and Dill, 2002). Its dorsal fin is closely similar in shape and size to that of *C. carcharias*, but the dermal fiber structure suggests greater flexibility, which, in my view, may create less resistance during the strong lateral movements involved in underwater shake feeding (Frazzetta, and Prange, 1987; Frazzetta, 1988, 1994), while stability is maintained by the pectoral fins (Springer, 1961).

In dolphins it is not known whether or not there is a system of fibers in the dorsal fin that is a continuum of the helical fibers of the body, which may function in a similar way to that postulated here for sharks. Such an investigation may shed light on why the dorsal fin of killer whales, *Orcinus orca*, irreversibly falls over sharply during captivity. The present study on sharks also offers a possible insight into how integumental fibers in the extinct, fast-swimming ichthyosaurs (Lingham-Soliar 1999, 2001) may have contributed to an efficient stabilizer, given the apparent absence of any other form of internal support in the dorsal fin.

LITERATURE CITED

Alexander RMcN. 1965. The lift produced by the heterocercal tail of Selachii. J Exp Biol 43:131–138.

Alexander RMcN. 1987. Bending of cylindrical animals with helical fibers in their skin or cuticle. J Theor Biol 124:97–110.

Axer H, v, Keyserlingk DG, Prescher A. 2001. Collagen fibers in linea alba and rectus sheaths. II. J Surg Res 96:127–134.

Bass AJ, Ballard JA. 1972. Buoyancy control in the shark *Odontaspis taurus* (Rafinesque). Copeia 1972:594–595.

Bennett MB, Ker RF, Alexander RMcN. 1987. Elastic properties of structures in the tail of cetaceans (*Phocaena* and *Lagenorhynchus*) and their effects on the energy costs of swimming. J Zool Lond 211:177–192.

Blake RW. 1983. Fish locomotion. Cambridge, UK: Cambridge University Press.

Blickhan R, Cheng J-Y. 1994. Energy storage by elastic mechanisms in the tail of large swimmers—a re-evaluation. J Theor Biol 168:315–321.

Boustany AM, Davis SF, Pyle P, Anderson SD, Le Boeuf BJ, Block B. 2002. Expanded niche for white sharks. Nature 415: 35–36.

Braun J, Reif W-E. 1985. Aquatic locomotion in fishes and tetrapods. N Jb Abh 169:307–322.

Burkitt HG, Young B, Heath JW. 1993. Wheater's functional histology. Edinburgh: Churchill Livingstone.

Cliff G, Dudley SFJ, Jury MR. 1996. Catches of white sharks in KwaZulu-Natal, South Africa and environmental influences. In: Klimley AP, Ainley DG, editors. Great white sharks: the biology of *Carcharodon carcharias*. San Diego: Academic Press. p 351–362.

Compagno LJV. 1984. FAO species catalogue (vol.4). Sharks of the world. An annotated and illustrated catalogue of shark species known to date. Part 1. Hexanchiformes to Lamniformes. FAO Fish Synop 125.

Cortés E. 1999. Standardized diet compositions and trophic levels of sharks. ICES J Mar Sci 56:707–717.

Donley JM, Dickson KA. 2000. Swimming kinematics of juvenile kawakawa tuna (*Euthynnus affinis*) and chub mackerel (*Scomber japonicus*). J Exp Biol 203:3103–3116.

Drucker EG, Lauder GV. 2001. Locomotor function of the dorsal fin in teleost fishes: experimental analysis of wake forces in sunfish. J Exp Biol 204:2943–2958.

Fergusson IK, Compagno LJV, Marks MA. 2000. Predation by white sharks *Carcharodon carcharias* (Chondrichthyes: Lamnidae) upon chelonians, with new records from the Mediterranean Sea and a first record of the ocean sunfish *Mola mola* (Osteichthyes: Molidae) as stomach contents. Environ Biol Fish 58:447–453.

Ferry LA, Lauder GV. 1996. Heterocercal tail function in leopard sharks: a three-dimensional kinematic analysis of two models. J Exp Biol 199:2253–2268.

Fish FE. 1998. Comparative kinematics and hydrodynamics of odontocete cetaceans: morphological and ecological correlates with swimming performance. J Exp Biol 201:2867–2877.

Fish FE. 2002. Balancing requirements for stability and maneuverability in cetaceans. Integ Comp Biol 42:85–93.

Fish FE, Hui CA. 1991. Dolphin swimming—a review. Mamm Rev 21:181–195.

Fish FE, Peacock JE, Rohr JJ. 2003. Stabilization mechanism in swimming odontocete cetaceans by phased movements. Mar Mamm Sci 19:515–528.

Frazzetta TH. 1988. The mechanics of cutting and the form of shark teeth (Chondrichthyes, Elasmobranchii). Zoomorphology 108:93–107.

Frazzetta TH. 1994. Feeding mechanisms in sharks and other elasmobranchs. Adv Comp Environ Physiol 18:31–57.

Frazzetta TH, Prange CD. 1987. Movements of cephalic components during feeding in some requiem sharks Carcharhiniformes: (Carcharhinidae). Copeia 1987:979–993.

Froese R, Pauly D. 2002. Fishbase. World Wide Web electronic publication, www.fishbase.org (13 October 2002).

Gans C, Parson T. 1964. A photographic atlas of shark anatomy. Chicago: University of Chicago Press.

Gordon JE. 1978. Structures. Harmondsworth: Penguin Books.

Graham JB, Dewar H, Lai NC, Lowell WR, Arce SM. 1990. Aspects of shark swimming performance determined using a large water tunnel. J Exp Biol 151:175–192.

Hebrank MR. 1980. Mechanical properties and locomotor functions of eel skin. Biol Bull 158:58–68.

Hebrank MR, Hebrank JH. 1986. The mechanics of fish skin: lack of an 'external tendon' role in two teleosts. Biol Bull 171:236–247.

Heithaus MR, Dill LM. 2002a. Habitat use and foraging behavior of tiger sharks (*Galeocerdo cuvier*) in a seagrass ecosystem. Mar Biol 140:37–248.

Heithaus MR, Dill LM. 2002b. Food availability and tiger shark predation risk influence bottlenose dolphin habitat use. Ecology 83:480–491.

Heithaus MR, Marshall DJ, Buhleier BM, Dill LM. 2001. Employing crittercam to study habitat use and behavior of large sharks. Mar Ecol Prog Ser 209:307–310.

Humason GL. 1979. Animal tissue techniques. San Francisco: WH Freeman.

Last PR, Stevens JD. 1994. Sharks and rays of Australia. CSIRO. Australia.

Lighthill J. 1975. Mathematical biofluid dynamics. Philadelphia: Soc Industr Appl Maths.

Lingham-Soliar T. 1999. Rare soft tissue preservation showing fibrous structures in an ichthyosaur from the Lower Lias (Jurassic) of England. Proc R Soc Lond B 266:2367–2373.

Lingham-Soliar T. 2001. The ichthyosaur integument: skin fibers, a means for a strong, flexible and smooth skin. Lethaia 34:287–302.

Lingham-Soliar T, Reif W-E. 1998. Taphonomic evidence for fast tuna-like swimming in Jurassic and Cretaceous ichthyosaurs. N Jb Abh 207:171–183.

McGowan CA. 1999. A practical guide to vertebrate mechanics. Cambridge, UK: Cambridge University Press.

Moss SA. 1972. The feeding mechanism of sharks of the family Carcharinidae. J Zool Lond 167:123–136.

Motta PJ. 1977. Anatomy and functional morphology of dermal collagen fibers in sharks. Copeia 1977:454–464.

Naresh MD, Arumugam V, Sanjeevi R. 1997. Mechanical behaviour of shark skin. J Biosci 22:431–437.

Nauen JC, Lauder GV. 2002. Hydrodynamics of caudal fin locomotion by chub mackerel, *Scomber japonicus* (Scombridae). J Exp Biol 205:1709–1724.

Pabst DA. 1996a. Morphology of the subdermal connective sheath of dolphins: a new fiber-wound, thin-walled, pressurized cylinder model for swimming vertebrates. J Zool Lond 238:35–52.

Pabst DA. 1996b. Springs in swimming animals. Am Zool 36:723–735.

Pabst DA. 2000. To bend a dolphin: convergence of force transmission designs in cetaceans and scombrid fishes. Am Zool 40:146–155.

Randall JE. 1983. Size of the great white shark (*Carcharodon*). Science 181:169–170.

Reif W-E, Weishampel D. 1986. Anatomy and mechanics of the lunate tail in lamnid sharks. Zool Jb Anat 114:221–234.

Springer S. 1961. Dynamics of the feeding mechanism of large galeoid sharks. Am Zool 1:185–193.

Thomson KS. 1976. On the heterocercal tail in sharks. Paleobiology 2:19–38.

Thomson KS. Simanek DE. 1977. Body form and locomotion in sharks. Am Zool 17:343–354.

Tricas TC, McCosker JE. 1984. Predatory behavior of the white shark (*Carcharodon carcharias*), with notes on its biology. Proc Calif Acad Sci 43:221–238.

Tricas TC, Taylor LR, Naftel G. 1981. Diel behavior of the tiger shark, *Galeocerdo cuvier*, at French Frigate Shoals, Hawaiian Islands. Copeia 1981:904–908.

Veronda DR, Westman RA. 1970. Finite deformations of skin. J Biomech 3:111–124.

Vincent JFV. 1990. Structural biomaterials (revised edition). Princeton, NJ: Princeton University Press.

Vincent JFV, Jeronimidis G, Topping BHV, Khan AI. 1991. The mechanical design of skin—towards the development of new materials. In: Natural structures, principles, strategies and models in architecture. Sondersforschungbereif 230:165–170.

Wainwright SA, Biggs WD, Currey JD, Gosline JM. 1976. Mechanical design in organisms. London: Edward Arnold.

Wainwright SA, Vosburgh F, Hebrank JH. 1978. Shark skin: function in locomotion. Science 202:747–749.

Webb PW. 1983. Speed, acceleration and maneuverability of two teleost fishes. J Exp Biol 102:115–122.

Webb PW. 1984. Form and function in fish swimming. Sci Am 251:58–68.

Webb PW, Weihs D. 1983. Optimization of locomotion. In: Webb P, Weihs D, editors. Fish biomechanics. New York: Praeger. p 339–371.

Weihs D. 1993. Stability of aquatic animal locomotion. Cont Math 141:443–461.